Journal of Thermal Stresses

ISSN: 0149-5739 (Print) 1521-074X (Online) Journal homepage: http://www.tandfonline.com/loi/uths20

# Thermal post-buckling behavior of simply supported sandwich panels with truss cores

Wu Yuan, Hongwei Song & Chenguang Huang

**To cite this article:** Wu Yuan, Hongwei Song & Chenguang Huang (2016) Thermal post-buckling behavior of simply supported sandwich panels with truss cores, Journal of Thermal Stresses, 39:2, 156-169

**To link to this article:** http://dx.doi.org/10.1080/01495739.2015.1123963

Published online: 09 Feb 2016.

JOURNAL OF THERMAL STRESSES
2016, VOL. 39, NO. 2, 156–169
http://dx.doi.org/10.1080/01495739.2015.1123963

Taylor & Francis
Taylor & Francis Group

# Thermal post-buckling behavior of simply supported sandwich panels with truss cores

Wu Yuan, Hongwei Song, and Chenguang Huang

Key Laboratory for Mechanics in Fluid Solid Coupling Systems, Institute of Mechanics, Chinese Academy of Sciences, Beijing, China

**ABSTRACT**

This article presents a thermal post-buckling solution for sandwich panels with truss cores under simply supported conditions, when subjected to uniform temperature rise. The Reissner assumptions are adopted and truss cores are assumed to be continuous and homogeneous. Differential governing equations are developed based on the variational principle. The perturbation technique is employed to determine the thermal post-buckling path of sandwich panels with truss cores. Based on the present method, influences of truss core configuration, relative density, aspect ratio, and initial imperfection on the thermal post buckling behavior are discussed.

**ARTICLE HISTORY**
Received 10 February 2015
Accepted 12 October 2015

**KEYWORDS**
Perturbation technique; sandwich panel; thermal post-buckling; truss cores

## Introduction

Sandwich panels with truss cores (SPTCs) have been considered to be promising candidates for load bearing components and thermal protection systems (TPS) in high speed flights, due to the superior characteristics such as high specific strength, high specific stiffness and multifunctional properties. When being used in TPS, the SPTC typically experiences large non-uniform temperature rise and may buckle due to thermal stresses. Therefore, the prediction of the thermal buckling response of the SPTC becomes of utmost importance, in order to integrate this novel lightweight and multifunctional structure into a flight-ready aircraft. In recent years, SPTCs have been extensively investigated on their fundamental properties, thermal insulation, shock resistance and energy absorption behaviors [1–12]. However, the post-buckling behavior of SPTCs under thermal loadings, which is quite different from conventional panels and may demonstrate unique properties, have not been systematically studied.

There have been a wealthy of theoretical works on the prediction of the critical buckling temperature (CBT) for plates and laminates. Based on the first-order shear deformation theory, Kabir et al. [13] obtained the CBT of clamped rectangular plates with symmetric angle-ply lamination. Kant and Babu [14] analyzed the buckling behavior of skew fibre-reinforced composites and sandwich plates by using shear deformable finite element models. Mansourand Shariyat [15] obtained the CBT of the functionally graded orthotropic plates by using a new differential quadrature method. Since plates and laminates always have initial imperfections, there also have some theoretical and numerical analysis on the thermal post-buckling behaviors. Mossavarali and Eslami [16] studied the thermal post-buckling behavior of thin plates which has initial flaws.

Based on the classical thin plate theory, Singh et al. [17] studied the thermal post-buckling behavior of rectangular antisymmetric cross-ply composite plate by using the Rayleigh-Ritz method. Thankam et al. [18] analyzed the thermal post-buckling behavior of laminated plates by using the finite element method. Sohn and Kim [19] used finite element method to calculate the thermal post-buckling response of functionally graded panels subjected to combined thermal and aerodynamic loads. Shen [20] analyzed

**CONTACT** Hongwei Song songhw@imech.ac.cn Key Laboratory for Mechanics in Fluid Solid Coupling Systems, Institute of Mechanics, Chinese Academy of Sciences, No. 15 Beisihuanxi Road, Beijing 100190, China.
Color versions of one or more of the figures in the article can be found online at www.tandfonline.com/uths.

the thermal post-buckling behavior of shear deformable functionally graded plates with temperature-depended properties by using a two-step perturbation technique.

For SPTCs that have weak cores and strong facesheets, the transverse shear deformation is mainly produced by the truss cores and should not be neglected. Therefore, the SPTC cannot be simplified as a thick plate or a laminate. To obtain the CBT of the SPTC, Chen et al. [21] solved the characteristic equations of simply supported SPTC under uniform thermal loading based on the Reissner model [22]. Yuan et al. [23] obtained CBTs of SPTCs under fully clamped boundary conditions by using double Fourier expansions to the virtual deformation mode. Later on, Yuan et al. [24] also performed experimental study on the thermal buckling behavior of SPTCs under uniform high temperature environments, and captured the full-field deformation history through the revised noncontact three-dimensional digital image correlation technique. It is found that the sandwich panel deformed in asymmetric mode in high temperature environments, due to fabrication defects. However, there have been few theoretical works on the thermal post-buckling behavior of the SPTC.

The present work focuses on the thermal post-buckling behavior of simply supported SPTCs subjected to uniform thermal loading. To obtain the buckling deformation of SPTCs, the truss core is assumed to be a continuous material. For the equivalent mechanical behavior, Deshpande et al. [25] gave the three-dimensional elastic constitutive relationship of lattice truss cores. Hyun et al. [26] obtained the properties of Kagome and tetragonal truss cores by using the finite element method. In general, the equivalent mechanical properties of truss cores are derived by geometric deformation of the lattice truss cells. Subsequently the governing differential equations of SPTCs with initial imperfection are obtained by using the variational principle. The thermal post-buckling equilibrium path is obtained by using the perturbation method. Structure parameters that affect the thermal post-buckling response of SPTCs are also discussed.

## Theory and formulation

In the present study, a simply supported SPTC subjected to uniform thermal loading is considered. The most commonly investigated configurations of truss cores are pyramidal, tetrahedral and Kagome, which are illustrated in Figures 1a and 1b. The equivalent analytical model is shown in Figure 1c. In the Cartesian coordinate system, the $OXY$ plane is located in accordance with the middle plane of the SPTC, and the edge lengths of the SPTC along the $X$ and $Y$ directions are $a$ and $b$, respectively. The thicknesses of the truss core and SPTC along the $Z$ direction are $h_p$ and $h_c$, respectively. For the SPTC, the buckling deformation is small and the major deformation is produced by the facesheet. In addition, the deformations of the facesheet and truss core are compatible and continuous. Therefore, the rotation of the truss can be neglected. To obtain the theoretical model, the following assumptions are made:

(1) The size of the unit truss cell is small in comparison with the size of the SPTC, therefore the truss core is considered as a continuous and homogeneous material.
(2) The truss is pin-jointed at the core-facesheet interface; therefore, the truss core does not contribute to the overall flexural rigidity.
(3) The transverse shear stiffness of the SPTC is only contributed by the truss core.

Due to the thin facesheet and the soft truss core, the shear deformation of SPTC is mainly produced by the truss core, and the transverse shear deformation of the facesheet can be neglected. Therefore, the first-order deformation theory is adopted. Strains of the facesheet are given by [16]

$$\begin{aligned}
\varepsilon_X &= \frac{\partial U}{\partial X} + \frac{1}{2}\left(\frac{\partial W}{\partial X}\right)^2 + \frac{\partial W}{\partial X}\frac{\partial W_0}{\partial X} + Z\left(\frac{\partial \psi_X}{\partial X}\right) \\
\varepsilon_Y &= \frac{\partial V}{\partial Y} + \frac{1}{2}\left(\frac{\partial W}{\partial Y}\right)^2 + \frac{\partial W}{\partial Y}\frac{\partial W_0}{\partial Y} + Z\left(\frac{\partial \psi_Y}{\partial Y}\right) \\
\varepsilon_{XY} &= \frac{1}{2}\left(\frac{\partial U}{\partial Y} + \frac{\partial V}{\partial X} + \frac{\partial W}{\partial X}\frac{\partial W}{\partial Y} + \frac{\partial W_0}{\partial X}\frac{\partial W}{\partial Y} + \frac{\partial W}{\partial X}\frac{\partial W_0}{\partial Y} + Z\left(\frac{\partial \psi_X}{\partial Y} + \frac{\partial \psi_Y}{\partial X}\right)\right)
\end{aligned} \tag{1}$$

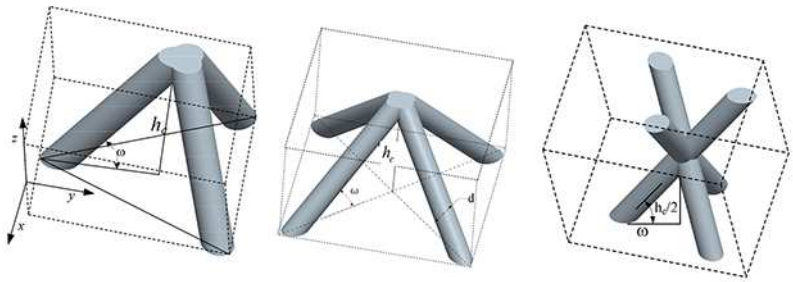

(a) Representative unit element of truss core: tetrahedral, pyramidal and Kagome

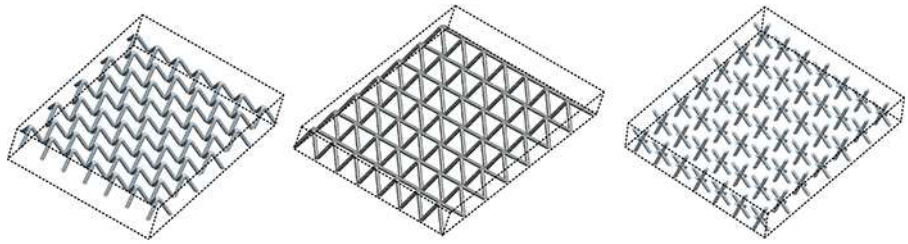

(b) truss core: tetrahedral, pyramidal and Kagome configuration

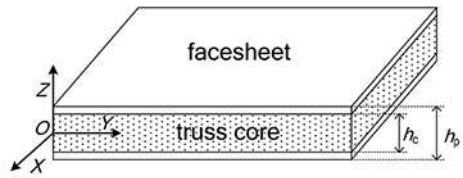


(c) Equivalent analytical model

**Figure 1.** Theoretical analysis model of SPTC.

The equivalent strains of truss cores can be expressed as

$$\begin{aligned} \varepsilon_{XZ} &= \frac{1}{2}\left(\psi_X + \frac{\partial W}{\partial X}\right) \\ \varepsilon_{YZ} &= \frac{1}{2}\left(\psi_Y + \frac{\partial W}{\partial Y}\right) \end{aligned} \tag{2}$$

where $U$, $V$ and $W$ are displacements of the middle plane of the SPTC in the $X$, $Y$, and $Z$ directions, while $\psi_X$ and $\psi_Y$ are rotations of the normal to the $XZ$ and $YZ$ planes, respectively. Additionally, $W_0$ is the initial geometric imperfection of the SPTC.

According to Hooke's law, stresses in the facesheet are expressed as

$$\begin{aligned} \sigma_X &= \frac{E}{1-\mu^2}(\varepsilon_X + \mu\varepsilon_Y - (1+\mu)\alpha\Delta T) \\ \sigma_Y &= \frac{E}{1-\mu^2}(\varepsilon_Y + \mu\varepsilon_X - (1+\mu)\alpha\Delta T) \\ \tau_{XY} &= \frac{E}{1+\mu}\varepsilon_{XY} \end{aligned} \tag{3}$$

And stresses in the truss core are written as

$$\begin{aligned} \tau_{XZ} &= 2G_c\varepsilon_{XZ} \\ \tau_{YZ} &= 2G_c\varepsilon_{YZ} \end{aligned} \tag{4}$$

where $E$ and $\mu$ are the elastic modulus and Poisson's ratio of the facesheet respectively. $G_c$ is the equivalent shear modulus of truss core, which is obtained by using the representative unit cell approach. $\alpha$ and $\Delta T$ are the coefficient of thermal expansion of the facesheet and the temperature rise, respectively.

The strain energy of the facesheet and the truss core are

$$\begin{aligned} u_{\text{factsheet}} &= \frac{1}{2}\iiint_{v_{\text{factsheet}}} (\sigma_X\varepsilon_X + \sigma_Y\varepsilon_Y + 2\tau_{XY}\varepsilon_{XY})\, dXdYdZ \\ u_{\text{core}} &= \iiint_{v_{\text{core}}} (\tau_{XZ}\varepsilon_{XZ} + \tau_{YZ}\varepsilon_{YZ})\, dXdYdZ \end{aligned} \tag{5}$$

According to the minimum potential energy principle

$$\delta u = \delta u_{\text{factsheet}} + \delta u_{\text{core}} = 0 \tag{6}$$

by using $U$, $V$, $W$, $\psi_X$, $\psi_Y$ as independent variables, the governing differential equations can be deduced

$$\begin{aligned} &\frac{\partial N_X}{\partial X} + \frac{\partial N_{XY}}{\partial Y} = 0 \\ &\frac{\partial N_{XY}}{\partial X} + \frac{\partial N_Y}{\partial Y} = 0 \\ &\frac{\partial Q_X}{\partial X} + \frac{\partial Q_Y}{\partial Y} + \frac{\partial}{\partial X}\left(N_X\frac{\partial(W+W_0)}{\partial X} + N_{XY}\frac{\partial(W+W_0)}{\partial Y}\right) \\ &\quad + \frac{\partial}{\partial Y}\left(N_{XY}\frac{\partial(W+W_0)}{\partial X} + N_Y\frac{\partial(W+W_0)}{\partial Y}\right) = 0 \\ &\frac{\partial M_X}{\partial X} + \frac{\partial M_{XY}}{\partial Y} - Q_X = 0 \\ &\frac{\partial M_{XY}}{\partial X} + \frac{\partial M_Y}{\partial Y} - Q_Y = 0 \end{aligned} \tag{7}$$

It is assumed that the SPTC is subjected to uniform thermal loading. In this case, the internal force can be expressed as

$$\begin{aligned} N_X &= \frac{E(h_p - h_c)}{1-\mu^2}\left(\frac{\partial U}{\partial X} + \frac{1}{2}\left(\frac{\partial W}{\partial X}\right)^2 + \frac{\partial W}{\partial X}\frac{\partial W_0}{\partial X} + \mu\left(\frac{\partial V}{\partial Y} + \frac{1}{2}\left(\frac{\partial W}{\partial Y}\right)^2 + \frac{\partial W}{\partial Y}\frac{\partial W_0}{\partial Y}\right) - (1+\mu)\alpha\Delta T\right) \\ N_Y &= \frac{E(h_p - h_c)}{1-\mu^2}\left(\frac{\partial V}{\partial Y} + \frac{1}{2}\left(\frac{\partial W}{\partial Y}\right)^2 + \frac{\partial W}{\partial Y}\frac{\partial W_0}{\partial Y} + \mu\left(\frac{\partial U}{\partial X} + \frac{1}{2}\left(\frac{\partial W}{\partial X}\right)^2 + \frac{\partial W}{\partial X}\frac{\partial W_0}{\partial X}\right) - (1+\mu)\alpha\Delta T\right) \\ N_{XY} &= G\left(h_p - h_c\right)\left(\frac{\partial U}{\partial Y} + \frac{\partial V}{\partial X} + \frac{\partial W}{\partial X}\frac{\partial W}{\partial Y} + \frac{\partial W_0}{\partial X}\frac{\partial W}{\partial Y} + \frac{\partial W}{\partial X}\frac{\partial W_0}{\partial Y}\right) \\ M_X &= D\left(\frac{\partial \psi_X}{\partial X} + \mu\left(\frac{\partial \psi_Y}{\partial Y}\right)\right), M_Y = D\left(\frac{\partial \psi_Y}{\partial Y} + \mu\left(\frac{\partial \psi_X}{\partial X}\right)\right), M_{XY} = \frac{(1-\mu)D}{2}\left(\frac{\partial \varphi_X}{\partial Y} + \frac{\partial \varphi_Y}{\partial X}\right) \\ Q_X &= C\left(\psi_X + \frac{\partial W}{\partial X}\right), \quad Q_Y = C\left(\psi_Y + \frac{\partial W}{\partial Y}\right) \\ D &= \frac{E(h_p^3 - h_c^3)}{12(1-\mu^2)}, \quad C = G_c h_c \end{aligned} \tag{8}$$

where $C$ and $D$ are the shear stiffness and flexural rigidity of the SPTC, respectively.

In addition, the deformation compatibility equation and stress functions are considered

$$N_X = \frac{\partial^2 \overline{F}}{\partial Y^2}, \quad N_Y = \frac{\partial^2 \overline{F}}{\partial X^2}, \quad N_{XY} = -\frac{\partial^2 \overline{F}}{\partial X \partial Y}$$
$$\frac{\partial^2 \varepsilon_X}{\partial Y^2} + \frac{\partial^2 \varepsilon_Y}{\partial X^2} - \frac{\partial^2 \varepsilon_{XY}}{\partial X \partial Y} = \left(\frac{\partial^2 W}{\partial X \partial Y}\right)^2 - \frac{\partial^2 W}{\partial X^2}\frac{\partial^2 W}{\partial Y^2} + 2\frac{\partial^2 W}{\partial X \partial Y}\frac{\partial^2 W_0}{\partial X \partial Y} - \frac{\partial^2 W}{\partial X^2}\frac{\partial^2 W_0}{\partial Y^2} - \frac{\partial^2 W}{\partial Y^2}\frac{\partial^2 W_0}{\partial X^2} \tag{9}$$

Before proceeding, it is convenient to define the following dimensionless quantities in the differential governing equations

$$x = \frac{\pi X}{a}, \quad y = \frac{\pi Y}{b}, \quad \beta = \frac{a}{b}, \quad w = \frac{W}{h_p}\sqrt{12(1-\mu^2)}$$
$$w_0 = \frac{W_0}{h_\mathrm{p}}\sqrt{12(1-\mu^2)}, \quad F = \frac{\overline{F}}{D}, \quad \gamma^2 = \frac{h_\mathrm{p}^2(h_\mathrm{p}-h_\mathrm{c})}{h_\mathrm{p}^3 - h_\mathrm{c}^3}$$
$$\varphi_x = \frac{a\psi_X}{\pi h_\mathrm{p}}\sqrt{12(1-\mu^2)}, \quad \varphi_y = \frac{a\psi_Y}{\pi h_\mathrm{p}}\sqrt{12(1-\mu^2)}, \quad \phi^2 = \frac{\pi^2}{b^2}\left(\frac{D}{C}\right), \quad \eta^2 = \frac{\pi^2}{a^2}\left(\frac{D}{C}\right) \tag{10}$$
$$\xi = \frac{12a^2(1-\mu^2)}{\pi^2 h_\mathrm{p}^2}, \quad \delta_x = \xi\bar{\delta}_X, \quad \delta_y = \xi\bar{\delta}_Y$$

Therefore the nonlinear differential governing equations of the thermal post-buckling of SPTC in the dimensionless form can be obtained

$$\begin{aligned}
&\bar{\nabla}^4 F = \beta^2\gamma^2\left(\left(\frac{\partial^2 w}{\partial x \partial y}\right)^2 - \frac{\partial^2 w}{\partial x^2}\frac{\partial^2 w}{\partial y^2} + 2\frac{\partial^2 w_0}{\partial x \partial y}\frac{\partial^2 w}{\partial x \partial y} - \frac{\partial^2 w}{\partial x^2}\frac{\partial^2 w_0}{\partial y^2} - \frac{\partial^2 w}{\partial y^2}\frac{\partial^2 w_0}{\partial x^2}\right)\\
&\frac{\partial \varphi_x}{\partial x} + \beta\frac{\partial \varphi_y}{\partial y} + \bar{\nabla}^2 w + \phi^2\frac{\partial}{\partial x}\left(\frac{\partial^2 F}{\partial y^2}\frac{\partial(w+w_0)}{\partial x} - \frac{\partial^2 F}{\partial x \partial y}\frac{\partial(w+w_0)}{\partial y}\right)\\
&\quad + \phi^2\frac{\partial}{\partial y}\left(\frac{\partial^2 F}{\partial x^2}\frac{\partial(w+w_0)}{\partial y} - \frac{\partial^2 F}{\partial x \partial y}\frac{\partial(w+w_0)}{\partial x}\right) = 0\\
&\eta^2\left(\frac{\partial^2 \varphi_x}{\partial x^2} + \mu\beta\frac{\partial^2 \varphi_y}{\partial x \partial y}\right) + \frac{(1-\mu)\eta^2}{2}\left(\beta^2\frac{\partial^2 \varphi_x}{\partial y^2} + \beta\frac{\partial^2 \varphi_y}{\partial x \partial y}\right) - \varphi_x - \frac{\partial w}{\partial x} = 0\\
&\eta^2\left(\beta^2\frac{\partial^2 \varphi_y}{\partial y^2} + \mu\beta\frac{\partial^2 \varphi_x}{\partial x \partial y}\right) + \frac{(1-\mu)\eta^2}{2}\left(\frac{\partial^2 \varphi_y}{\partial x^2} + \beta\frac{\partial^2 \varphi_x}{\partial x \partial y}\right) - \varphi_y - \beta\frac{\partial w}{\partial y} = 0
\end{aligned} \tag{11}$$

where

$$\bar{\nabla}^2 = \frac{\partial^2}{\partial x^2} + \beta^2\frac{\partial^2}{\partial y^2}$$
$$\bar{\nabla}^4 = \frac{\partial^4}{\partial x^4} + 2\beta^2\frac{\partial^2}{\partial x^2 \partial y^2} + \beta^4\frac{\partial^4}{\partial y^4}$$

The simply supported boundary conditions are

$$\begin{aligned}
&x = 0 \text{ and } x = \pi : w = \varphi_y = 0, \quad \frac{\partial^2 F}{\partial x \partial y} = M_x = 0\\
&y = 0 \text{ and } y = \pi : w = \varphi_x = 0, \quad \frac{\partial^2 F}{\partial x \partial y} = M_y = 0
\end{aligned} \tag{12}$$

And the end-shorting relationships can be expressed as [27]

$$\begin{aligned}\delta_x &= \int\int \frac{\partial u}{\partial x}dxdy = \int\int \left(\frac{1}{\gamma^2}\left(\frac{\partial^2 F}{\partial x^2} - \mu\beta^2\frac{\partial^2 F}{\partial y^2}\right) - \frac{1}{2}\left(\frac{\partial w}{\partial x}\right)^2 - \frac{\partial w}{\partial x}\frac{\partial w_0}{\partial x} + \xi\alpha\Delta T\right)dxdy \\ \delta_y &= \int\int \frac{\partial v}{\partial y}dxdy = \int\int \left(\frac{1}{\gamma^2}\left(\beta^2\frac{\partial^2 F}{\partial y^2} - \mu\frac{\partial^2 F}{\partial x^2}\right) - \frac{\beta^2}{2}\left(\frac{\partial w}{\partial y}\right)^2 - \beta^2\frac{\partial w}{\partial y}\frac{\partial w_0}{\partial y} + \xi\alpha\Delta T\right)dxdy\end{aligned} \tag{13}$$

## Asymptotic solutions

Applying Eq. (11), the buckling behavior of SPTC is determined by the two-step perturbation technique [20]. Solutions of unknown functions are assumed to have the following forms

$$\begin{aligned} w(x,y,\varepsilon) &= \sum_{i=1}\varepsilon^i w_i(x,y), \quad F(x,y,\varepsilon) = \sum_{i=0}\varepsilon^i F_i(x,y) \\ \varphi_x(x,y,\varepsilon) &= \sum_{i=1}\varepsilon^i \varphi_{xi}(x,y), \quad \varphi_y(x,y,\varepsilon) = \sum_{i=1}\varepsilon^i \varphi_{yi}(x,y)\end{aligned} \tag{14}$$

where $\varepsilon$ is a small perturbation parameter and the first term of out-of-plane displacement can be expressed as the classic solution of small deflection

$$w_1(x,y) = A_{11}\sin mx\sin ny \tag{15}$$

The initial geometric imperfection of the SPTC is assumed to have a similar form

$$w_0(x,y) = \varepsilon\lambda A_{11}\sin mx\sin ny \tag{16}$$

For the SPTC that has no initial geometric imperfection

$$\lambda = 0 \tag{17}$$

Substituting Eqs. (14)–(16) into Eq. (11) and collecting terms of the same order of $\varepsilon$, a set of perturbation equations is obtained. Unknown functions can be obtained by using the perturbation equations of each order. Finally, up to the fourth order, asymptotic solution are obtained

$$\begin{aligned} w(x,y,\varepsilon) &= \varepsilon\left[A_{11}\sin mx\sin ny\right] + \varepsilon^3\left[A_{13}\sin mx\sin 3ny + A_{31}\sin 3mx\sin ny\right] + O(\varepsilon^5) \\ \varphi_x(x,y,\varepsilon) &= \varepsilon\left[C_{11}\cos mx\sin ny\right] + \varepsilon^3\left[C_{13}\cos mx\sin 3ny + C_{31}\cos 3mx\sin ny\right] + O(\varepsilon^5) \\ \varphi_y(x,y,\varepsilon) &= \varepsilon\left[D_{11}\sin mx\cos ny\right] + \varepsilon^3\left[D_{13}\sin mx\cos 3ny + D_{31}\sin 3mx\cos ny\right] + O(\varepsilon^5)\end{aligned} \tag{18}$$

$$\begin{aligned} F(x,y,\varepsilon) = &-B_{100}\frac{y^2}{2} - b_{100}\frac{x^2}{2} + \varepsilon^2\left[-B_{200}\frac{y^2}{2} - b_{200}\frac{x^2}{2} + B_{220}\cos 2mx + B_{202}\cos 2ny\right] \\ &+ \varepsilon^4\Bigg[-B_{400}\frac{y^2}{2} - b_{400}\frac{x^2}{2} + B_{420}\cos 2mx + B_{402}\cos 2ny + B_{422}\cos 2mx\cos 2ny \\ &+ B_{440}\cos 4mx + B_{404}\cos 4ny + B_{424}\cos 2mx\cos 4ny + B_{442}\cos 4mx\cos 2ny\Bigg] + O(\varepsilon^5)\end{aligned}$$

where

$$\begin{aligned} C_{11} &= \frac{mk_{22} - \beta nk_{12}}{k_{11}k_{22} - k_{12}k_{21}}A_{11}, \quad D_{11} = \frac{\beta nk_{11} - mk_{21}}{k_{11}k_{22} - k_{12}k_{21}}A_{11} \\ A_{13} &= f_2(\zeta_{33}\zeta_{55} - \zeta_{35}\zeta_{53})/\chi_1, \quad A_{31} = f_1(\zeta_{44}\zeta_{66} - \zeta_{46}\zeta_{64})/\chi_2, \quad C_{13} = -f_2(\zeta_{31}\zeta_{55} - \zeta_{35}\zeta_{51})/\chi_1 \\ C_{31} &= -f_1(\zeta_{42}\zeta_{66} - \zeta_{46}\zeta_{62})/\chi_2, \quad D_{13} = f_2(\zeta_{31}\zeta_{53} - \zeta_{33}\zeta_{51})/\chi_1, \quad D_{31} = f_1(\zeta_{42}\zeta_{64} - \zeta_{44}\zeta_{62})/\chi_2 \\ B_{100} &= \frac{1}{\phi^2(1+\lambda)(m^2+n^2\beta^2)}\left(m\frac{mk_{11} - \beta nk_{12}}{k_{11}k_{22} - k_{12}k_{21}} + \beta n\frac{\beta nk_{11} - mk_{21}}{k_{11}k_{22} - k_{12}k_{21}} + m^2 + \beta^2 n^2\right), \\ b_{100} &= \beta^2 B_{100}\end{aligned}$$

$$
\begin{aligned}
B_{200} &= \frac{1}{m^2+n^2}\left(2m^2n^2\left(\frac{n^2(1+2\lambda)\beta^2\gamma^2}{32m^2}A_{11}^2+\frac{m^2(1+2\lambda)\gamma^2}{32n^2\beta^2}A_{11}^2\right)-\frac{(\gamma^2+2\lambda)(\beta^2n^2-m^2)}{8(1+\mu)}A_{11}^2\right)\\
b_{200} &= \beta^2B_{200}+\frac{(\gamma^2+2\lambda)(\beta^2n^2-m^2)}{8(1+\mu)}A_{11}^2,\quad B_{400}=\frac{2\phi^2m^2n^2(B_{202}A_{13}+B_{220}A_{31})}{A_{11}(1+\lambda)(m^2\phi^2+\beta^2n^2\phi^2)},b_{400}=\beta^2B_{400}\\
B_{420} &= -\frac{16n^2\beta^2\gamma^2(1+\lambda)A_{11}A_{31}}{m^2},\quad B_{422}=-\frac{4m^2n^2\beta^2\gamma^2(1+\lambda)A_{11}(A_{31}+A_{13})}{16m^4+32m^2n^2\beta^2+n^4\beta^4},\\
B_{440} &= -\frac{n^2\beta^2\gamma^2(1+\lambda)A_{11}A_{31}}{64m^2}\\
B_{424} &= -\frac{m^2n^2\beta^2\gamma^2(1+\lambda)A_{11}A_{13}}{16m^4+128m^2n^2\beta^2+256n^4\beta^4},\quad B_{442}=-\frac{m^2n^2\beta^2\gamma^2(1+\lambda)A_{11}A_{13}}{256m^4+128m^2n^2\beta^2+16n^4\beta^4}\\
B_{402} &= -\frac{m^2n^2\gamma^2(1+\lambda)A_{11}A_{31}}{16n^2\beta^2},\quad B_{404}=\frac{m^2n^2\gamma^2(1+\lambda)A_{11}A_{31}}{64n^2\beta^2}
\end{aligned}
\tag{19}
$$

and parameters in Eq. (19) can be expressed as

$$
\begin{aligned}
\chi_1 &= \zeta_{21}\zeta_{33}\zeta_{55}-\zeta_{21}\zeta_{35}\zeta_{53}-\zeta_{23}\zeta_{31}\zeta_{55}+\zeta_{23}\zeta_{35}\zeta_{51}+\zeta_{25}\zeta_{31}\zeta_{53}-\zeta_{25}\zeta_{33}\zeta_{51}\\
\chi_2 &= \zeta_{12}\zeta_{44}\zeta_{66}-\zeta_{12}\zeta_{46}\zeta_{64}-\zeta_{14}\zeta_{42}\zeta_{66}+\zeta_{14}\zeta_{46}\zeta_{62}+\zeta_{16}\zeta_{42}\zeta_{64}-\zeta_{16}\zeta_{44}\zeta_{62}\\
k_{11} &= -\frac{1}{2}(1-\mu)\beta^2n^2\eta^2-1-m^2\eta^2,\quad k_{12}=k_{21}=-\frac{1}{2}(1+\mu)\eta^2mn\beta,\\
k_{22} &= -\beta^2n^2\eta^2-1-\frac{1}{2}(1-\mu)m^2\eta^2\\
\zeta_{12} &= 9m^2\phi^2B_{100}+n^2\phi^2b_{100}-n^2\beta^2-9m^2,\quad \zeta_{14}=3m,\quad \zeta_{16}=\beta n\\
\zeta_{21} &= m^2\phi^2B_{100}+9n^2\phi^2b_{100}-9n^2\beta^2-m^2,\quad \zeta_{23}=m,\quad \zeta_{25}=3n\beta\\
\zeta_{31} &= -m,\quad \zeta_{33}=-m^2\eta^2-\frac{9}{2}(1-\mu)\eta^2\beta^2n^2-1,\\
\zeta_{35} &= \zeta_{53}{=}\zeta_{46}{=}\zeta_{64}=-3\eta^2mn\mu\beta-\frac{3}{2}(1-\mu)\eta^2mn\beta\\
\zeta_{42} &= -3m,\quad \zeta_{44}=-9m^2\eta^2-\frac{1}{2}(1-\mu)\eta^2\beta^2n^2-1\\
\zeta_{51} &= -3n\beta,\quad \zeta_{55}=-9\eta^2\beta^2n^2-\frac{1}{2}(1-\mu)\eta^2m^2-1\\
\zeta_{62} &= -n\beta,\quad \zeta_{66}=-\eta^2\beta^2n^2-\frac{9}{2}(1-\mu)\eta^2m^2-1\\
f_1 &= \frac{(1+2\lambda)(1+\lambda)\beta^2n^4\phi^2\gamma^2}{16}A_{11}^3,\quad f_2=\frac{(1+\lambda)(1+2\lambda)m^4\phi^2\gamma^2}{16\beta^2}A_{11}^3
\end{aligned}
\tag{20}
$$

In the present work, the global buckling behavior of SPTC is considered. The maximum out-of-plane displacement, which is assumed at point $x=\frac{\pi}{2m}, y=\frac{\pi}{2n}$, can be expressed as

$$
w_m = A_{11}\varepsilon+\varepsilon^3\left(A_{13}+A_{31}\right)+O(\varepsilon^5) \tag{21}
$$

Then the perturbation parameter can be obtained

$$
A_{11}\varepsilon = w_m+\left(\frac{(1+\lambda)(1+2\lambda)m^4\phi^2\gamma^2}{16\beta^2}\Lambda_{13}+\frac{(1+2\lambda)(1+\lambda)\beta^2n^4\phi^2\gamma^2}{16}\Lambda_{31}\right)w_m^3+O(w_m^5) \tag{22}
$$

where

$$
\begin{aligned}
\Lambda_{13} &= (\zeta_{33}\zeta_{55}-\zeta_{35}\zeta_{53})/\chi_1\\
\Lambda_{31} &= (\zeta_{44}\zeta_{66}-\zeta_{46}\zeta_{64})/\chi_2
\end{aligned}
$$

Substituting Eq. (18) into boundary conditions $\delta_x = 0, \delta_y = 0$, the thermal post-buckling equilibrium path can be obtained

$$\Omega_T = \Omega_{10} + \Omega_{12} w_m^2 + \Omega_{14} w_m^4 \tag{23}$$

where

$$\begin{aligned}
\Omega_T &= \xi \alpha \Delta T \\
\Omega_{10} &= \frac{(1-\mu)\beta^2}{\gamma^2 \phi^2 (1+\lambda)(m^2+n^2\beta^2)} \left( m \frac{mk_{11} - \beta n k_{12}}{k_{11}k_{22} - k_{12}k_{21}} + \beta n \frac{\beta n k_{11} - m k_{21}}{k_{11}k_{22} - k_{12}k_{21}} + m^2 + \beta^2 n^2 \right) \\
\Omega_{12} &= \frac{1}{8}(1+2\lambda)\, m^2 + \frac{1}{\gamma^2} \left( \frac{\beta^2(1-\mu)}{m^2+n^2} \left( 2m^2 n^2 \left( \frac{n^2(1+2\lambda)\beta^2\gamma^2}{32m^2} \right. \right. \right. \\
&\quad \left. \left. \left. + \frac{m^2(1+2\lambda)\gamma^2}{32n^2\beta^2} \right) - \frac{(\gamma^2+2\lambda)(\beta^2 n^2 - m^2)}{8(1+\mu)} \right) + \frac{(\gamma^2+2\lambda)(\beta^2 n^2 - m^2)}{8(1+\mu)} \right) \\
\Omega_{14} &= \frac{\beta^2(1-\mu)}{\gamma^2} \frac{2\phi^2 m^2 n^2}{(1+\lambda)(m^2\phi^2 + \beta^2 n^2 \phi^2)} \left( \frac{n^2(1+2\lambda)\beta^2\gamma^2}{32m^2} \frac{(1+\lambda)(1+2\lambda)m^4\phi^2\gamma^2}{16\beta^2} \Lambda_{13} \right. \\
&\quad \left. + \frac{m^2(1+2\lambda)\gamma^2}{32n^2\beta^2} \frac{(1+2\lambda)(1+\lambda)\beta^2 n^4 \phi^2 \gamma^2}{16} \Lambda_{31} \right) \\
&\quad + 2\Omega_{12} \left( \frac{(1+\lambda)(1+2\lambda)m^4\phi^2\gamma^2}{16\beta^2} \Lambda_{13} + \frac{(1+2\lambda)(1+\lambda)\beta^2 n^4 \phi^2 \gamma^2}{16} \Lambda_{31} \right)
\end{aligned}$$

## Results and discussions

In this section, the post-buckling behavior of the SPTC is obtained according to the theoretical model. The geometric parameters and material properties used in the theoretical analysis are listed in Table 1.

### *Comparison of CBTs with different theories*

To solve the CBT of SPTC, the small deflection theory may lead to desirable results. Figure 2 shows the comparison of CBTs of pyramidal SPTC obtained from the present theory with that from the small deflection theory [21, 23]. It can be found that CBTs from the present theory model are in good agreement with the small deflection theory. However, the linear small deflection theory may lead to significant errors due to the large amplitude thermal post-buckling deformations. Therefore, the nonlinear large deflection theory is used to get the thermal post-buckling response of SPTC.

### *Effects of initial geometric imperfection*

Figure 3 shows the effect of initial geometric imperfection on the thermal post-buckling behavior of SPTCs. Lines with $W_0/h_p = 0$ are thermal post-buckling equilibrium paths of SPTCs that do not have initial geometric imperfections, and $W_0/h_p = 0.05$ are equilibrium paths of imperfect SPTCs. For perfect SPTCs, there is no out-of-plane displacement when the temperature rise is under the CBT, whereas it increases dramatically when the temperature rise is larger than the CBT. Unlike the perfect SPTC, there is initial out-of-plane displacement and the displacement increases dramatically when the temperature rise is approaching to the CBT of the perfect SPTC. The out-of-plane displacement of SPTC with large imperfections is larger than those with small imperfections due to the influence of initial

**Table 1.** Parameters used to calculate the thermal post-buckling path theoretically.

| $h_c$ (mm) | $h_p$ (mm) | $E$ (GPa) | $\mu$ | $\alpha$ ($\times 10^{-6}$) | $a$ (mm) | $b$ (mm) |
|---|---|---|---|---|---|---|
| 8 | 10 | 200 | 0.3 | 17 | 300 | 300 |

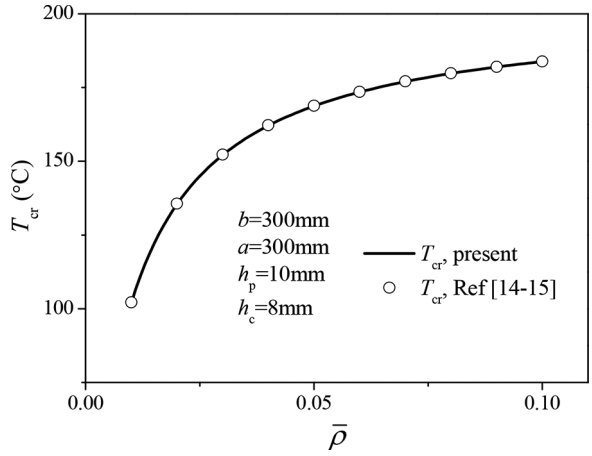


**Figure 2.** Comparisons of CBT predicted by different theories.

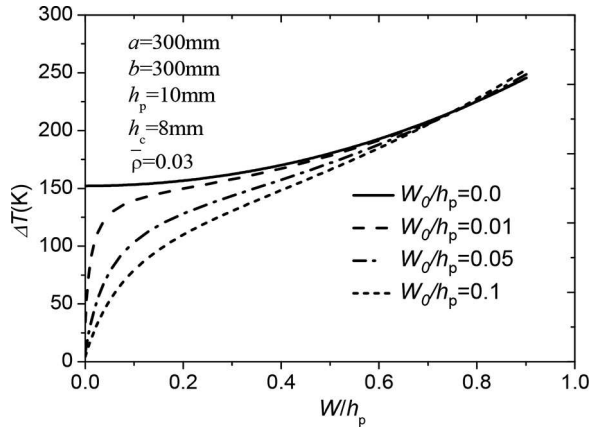


**Figure 3.** Effect of initial imperfection on the thermal post-buckling behavior of SPTC.

geometric imperfection, whereas all of them tend to be the same when the dimensionless displacement $W/h_p = 0.7$.

### *Effects of truss core configuration and relative density*

Figure 4 shows the effect of truss configurations on the thermal post-buckling behavior of SPTC. For the three configurations of truss cores illustrated in Figure 1a, the equivalent shear stiffness can be expressed as

$$\begin{aligned} C_{\text{pyramid}} &= G_{\text{pyramid}} h_c = \frac{1}{8}\overline{\rho} E h_c, \\ C_{\text{tet}} &= C_{\text{kagome}} = G_{\text{tet}} h_c = \frac{1}{9}\overline{\rho} E h_c \end{aligned} \tag{24}$$

where $C_{\text{pyramid}}$, $C_{\text{tet}}$ and $C_{\text{kagome}}$are the equivalent shear stiffness of the pyramidal, tetrahedral and Kagome truss cores, respectively. $G_{\text{pyramid}}$, $G_{\text{tet}}$ and $G_{\text{kagome}}$are the equivalent shear modulus of the pyramidal, tetrahedral and Kagome truss cores [23]. $\overline{\rho}$ is the relative density of the truss core. From Eq. (24), the shear stiffness of the pyramidal truss core is larger than the Kagome and tetrahedral cores, when they are in the same relative density. Therefore, the resistance to thermal post-buckling of a SPTC with pyramidal truss cores will be higher than those of the other two configurations. In addition, the

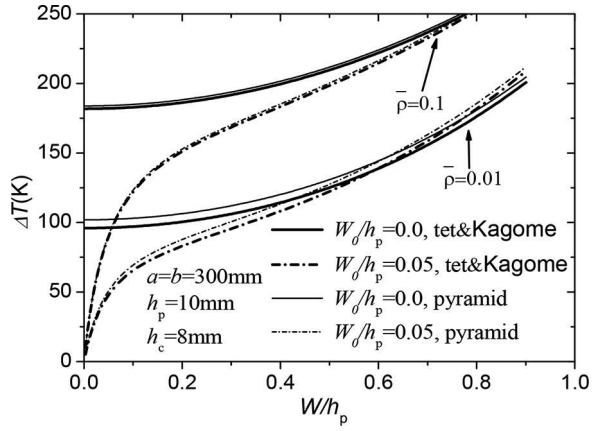


**Figure 4.** Effect of truss configuration on the thermal post-buckling behavior of SPTC.

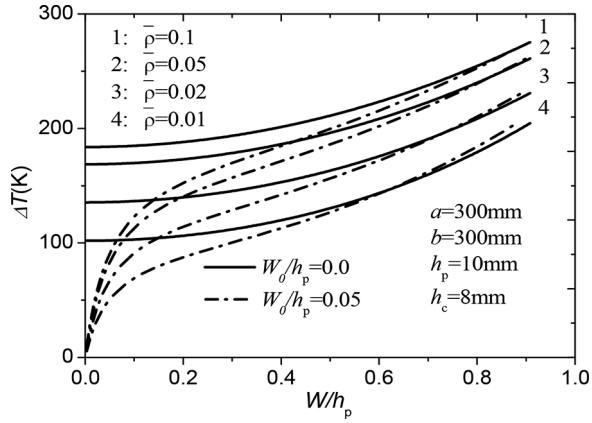


**Figure 5.** Effect of relative density of truss core on the thermal post-buckling behavior of SPTC.

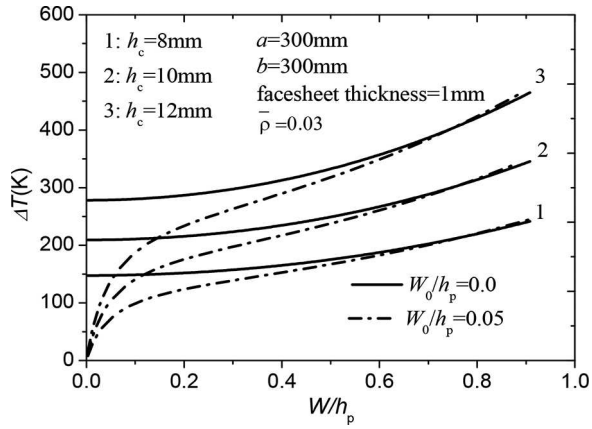


**Figure 6.** Effect of truss core thickness on the thermal post-buckling behavior.

difference is significant when the relative density is 0.01, but not so obvious when the relative density gets 0.1.

Figure 5 shows the thermal post-buckling behavior of pyramidal SPTC when the relative density of the truss core $\overline{\rho}$ is raised from 0.01 to 0.1. It can be seen that, the increase of relative density $\overline{\rho}$ yields

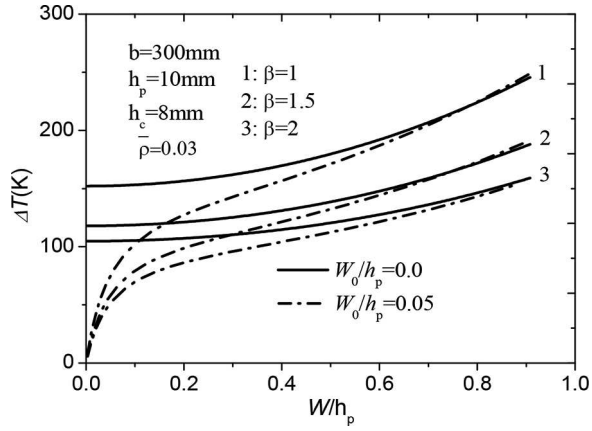


**Figure 7.** Effect of SPTC aspect ratio on the thermal post-buckling behavior.

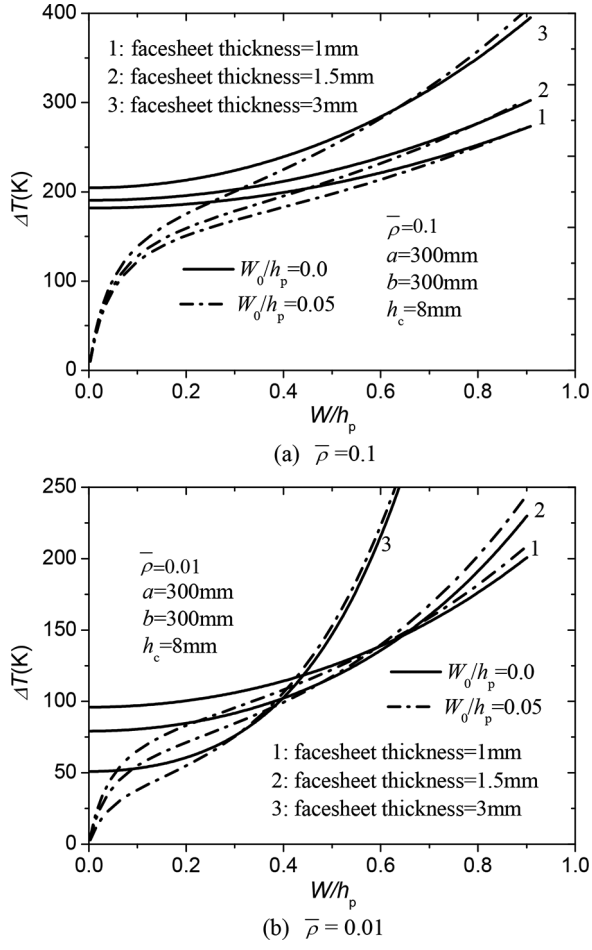


**Figure 8.** Effect of facesheet thickness on the thermal post-buckling behavior of SPTC.

an improved resistance of thermal post-buckling deformation. According to Eq. (24), the shear stiffness of the SPTC is directly related to the relative density. Therefore, the thermal post-buckling strength can be improved by using a higher relative density. However, according to Figure 2 and also ref. [23], the tendency slows down when the relative density is approaching to 0.06.

Figure 6 shows the effect of truss core thickness $h_c$ on the thermal post-buckling behavior of SPTC when the facesheet thickness is 1 mm and relative density is 0.03. When the truss core relative density $\overline{\rho}$ and the facesheet thickness are constant, the flexural rigidity grows dramatically as the truss core thickness is elevated. Therefore, the resistance to thermal post-buckling of SPTC is enhanced as the truss core thickness $h_c$ grows.

## Effects of aspect ratio and facesheet thickness

Figure 7 shows the effect of aspect ratio $\beta$ on the thermal post-buckling behavior of pyramidal SPTC when panel length $a$ is 300 mm. The increase in the width $b$ means the slenderness ratio of SPTC is increased, therefore, the CBT and thermal post-buckling resistance is decreased.

Both the in-plane load and the flexural stiffness of SPTC increase when the facesheet thickness is increased. As a result, the facesheet thickness has different effects on the thermal post-buckling resistance of SPTC when the truss core relative density $\overline{\rho}$ is varied. As Figure 8a shows, for the relative density $\overline{\rho} = 0.1$, the CBT and post-buckling resistance of SPTC are improved as the facesheet thickness is increased. When the relative density decreases to 0.01, as Figure 8b shows, the CBT decreases when the facesheet thickness is increased. However, the out-of-plane displacement of SPTC with smaller facesheet thickness is larger than that has bigger thickness when the temperature rise is increased.

## Conclusions

This article presents a theoretical analysis on the thermal post-buckling behavior of simply supported SPTC under uniform temperature rise. Based on the first-order shear deformation theory, the governing differential equations of SPTC are developed by using the variational principle. The CBT and the thermal post-buckling equilibrium path of SPTC are obtained by using the perturbation technique. CBTs calculated by the present model are in good agreement with that from the small deflection theory. Parameters that influence the post-buckling behavior of SPTC, including initial geometric imperfections, truss core configurations, relative densities, truss core thickness, aspect ratio, and facesheet thickness, are discussed. The resistance to thermal post-buckling of pyramidal SPTC is highest of the three configurations. The CBT and thermal post-buckling strength of SPTC can be improved by using a higher relative density. The stability of SPTC can be improved by adding the truss core thickness, but weakened when the length of SPTC increases. In addition, the effect of facesheet thickness on the CBT and thermal post-buckling resistance of SPTC is different when the relative density of the truss core is varied.

## Funding

Financial support from National Natural Science Foundation of China (Grant Nos. 11472276, 91016025, 11332011 and 91216303) and Funds of Science and Technology on Scramjet Laboratory are gratefully acknowledged.

## Nomenclature

| | |
|---|---|
| $a, b$ | Sandwich panel length |
| $C$ | Shear stiffness of sandwich panels |
| $D$ | Flexural rigidity of sandwich panels |
| $E$ | Modulus of the material |
| $F$ | Stress function in dimensionless units |
| $\overline{F}$ | Stress function |
| $G_c$ | Equivalent shear modulus of the lattice truss core |
| $h_c$ | Core thickness |
| $h_p$ | Sandwich panel thickness |
| $M_x$ | Bending moment in x-direction |
| $M_{xy}$ | Torsional moment |

| | |
|---|---|
| $M_y$ | Bending moment in y-direction |
| $N_x, N_y, N_{xy}$ | Compressive in-plane force |
| $Q_x, Q_y$ | Shear force |
| $U$ | Displacement in $X$-direction |
| $u$ | Displacement in $X$-direction in dimensionless units |
| $V$ | Displacement in $y$-direction |
| $v$ | Displacement in $Y$-direction in dimensionless units |
| $W$ | Displacement in $Z$-direction |
| $W_0$ | Initial geometric imperfection |
| $w$ | Displacement in $Z$-direction in dimensionless units |
| $w_0$ | Initial geometric imperfection in dimensionless units |
| $w_m$ | Maximum displacement in $z$-direction in dimensionless units |
| $\alpha$ | Coefficient of thermal expansion of the sandwich panel |
| $\Delta T$ | Temperature rise |
| $\delta_x, \delta_y$ | End-shorting of sandwich panel |
| $\varepsilon_X, \varepsilon_Y, \varepsilon_{XY}$ | Strains of facesheet |
| $\varepsilon_{XZ}, \varepsilon_{YZ}$ | Strains of truss cores |
| $\mu$ | Poisson's ratio |
| $\overline{\rho}$ | Relative density of sandwich panel |
| $\sigma_X, \sigma_Y, \tau_{XY}$ | Stress of facesheet |
| $\tau_{XZ}, \tau_{YZ}$ | Stress of truss cores |
| $\psi_X, \psi_Y$ | Rotations of the normal in the $XZ$ and $YZ$ planes |
| $\varphi_x, \varphi_y$ | Rotations of the normal in the $XZ$ and $YZ$ planes in dimensionless units |

## References


1. T. Kim, C. Y. Zhao, T. J. Lu, and H. P. Hodson, Convective Heat Dissipation with Lattice-Frame Materials, *Mechanics of Materials*, vol. 36, pp. 767–780, 2004.
2. V. S. Deshpande and N. A. Fleck, Collapse of Truss Core Sandwich Beams in 3-Point Bending, *International Journal of Solids and Structures*, vol. 38, pp. 6275–6305, 2001.
3. K. P. Dharmasena, H. N. Wadley, K. Williams, Z. Xue, and J. W. Hutchinson, Response of Metallic Pyramidal Lattice Core Sandwich Panels to High Intensity Impulsive Loading in Air, *International Journal of Impact Engineering*, vol. 38, pp. 275–289, 2011.
4. M. Li, L. Wu, L. Ma, B. Wang, and Z. Guan, Structural Response of All-composite Pyramidal Truss Core Sandwich Columns in End Compression, *Composite Structures*, vol. 93, pp. 1964–1972, 2011.
5. X. M. Lu, Y. F. Ma, and S. X. Wang, The Study of Low-Velocity Impact Characteristics and Residual Tensile Strength of Carbon Fiber Composite Lattice Core Sandwich Structures, *Advanced Engineering Materials*, vol. 194–196, pp. 117–120, 2011.
6. J. S. Park, J. H. Joo, B. C. Lee, and K. J. Kang, Mechanical Behaviour of Tube-woven Kagome Truss Cores under Compression, *International Journal of Mechanical Sciences*, vol. 53, pp. 65–73, 2011.
7. S. Pingle, N. Fleck, V. Deshpande, and H. Wadley, Collapse Mechanism Maps for a Hollow Pyramidal Lattice, *Proceedings of the Royal Society A: Mathematical, Physical and Engineering Science*, vol. 467, pp. 985–1011, 2011.
8. D. Queheillalt, V. Deshpande, and H. Wadley, Truss Waviness Effects in Cellular Lattice Structures, *Journal of Mechanics of Materials and Structures*, vol. 2, pp. 1657–1675, 2007.
9. D. T. Queheillalt and H. N. Wadley, Titanium Alloy Lattice Truss Structures, *Materials and Design*, vol. 30, pp. 1966–1975, 2009.
10. B. Wang, L. Z. Wu, L. Ma, and J. C. Feng, Low-Velocity Impact Characteristics and Residual Tensile Strength of Carbon Fiber Composite Lattice Core Sandwich Structures, *Composites Part B-Engineering*, vol. 42, pp. 891–897, 2011.
11. N. Wicks and J. W. Hutchinson, Optimal Truss Plates, *International Journal of Solids and Structures*, vol. 38, pp. 5165–5183, 2001.
12. C. J. Yungwirth, H. N. G. Wadley, J. H. O'Connor, A. J. Zakraysek, and V. S. Deshpande, Impact Response of Sandwich Plates with a Pyramidal Lattice Core, *International Journal of Impact Engineering*, vol. 35, pp. 920–936, 2008.
13. H. R. H. Kabir, M. A. M. Hamad, J. Al-Duaij, and M. J. John, Thermal Buckling Response of All-Edge Clamped Rectangular Plates with Symmetric Angle-Ply Lamination, *Composite Structures*, vol. 79, pp. 148–155, 2007.
14. T. Kant and C. S. Babu, Thermal Buckling Analysis of Skew Fibre-Reinforced Composite and Sandwich Plates Using Shear Deformable Finite Element Models, *Composite Structures*, vol. 49, pp. 77–85, 2000.

15. M. H. Mansouri and M. Shariyat, Thermal Buckling Predictions of Three Types of High-Order Theories for the Heterogeneous Orthotropic Plates, Using the New Version of DQM, *Composite Structures*, vol. 113, pp. 40–55, 2014.
16. A. Mossavarali and M. R. Eslami, Thermoelastic Buckling of Plates with Imperfections Based on a Higher Order Displacement Field, *Journal of Thermal Stresses*, vol. 25, pp. 745–771, 2002.
17. G. Singh, G. V. Rao, and N. G. R. Iyengar, Thermal Post-buckling Behavior of Rectangular Antisymmetric Cross-Ply Composite Plates, *Acta Mechanica*, vol. 98, pp. 39–50, 1993.
18. V. S. Thankam, G. Singh, G. V. Rao, and A. K. Rath, Thermal Post-Buckling Behaviour of Laminated Plates Using a Shear-Flexible Element Based on Coupled-Displacement Field, *Composite Structures*, vol. 59, pp. 351–359, 2003.
19. K. J. Sohn and J. H. Kim, Structural Stability of Functionally Graded Panels Subjected to Aero-thermal Loads, *Composite Structures*, vol. 82, pp. 317–325, 2008.
20. H. S. Shen, Thermal Postbuckling Behavior of Shear Deformable FGM Plates with Temperature-Dependent Properties, *International Journal of Mechanical Sciences*, vol. 49, pp. 466–478, 2007.
21. J. W. Chen, Y. Q. Liu, W. Liu, and X. Y. Su, Thermal Buckling Analysis of Truss-core Sandwich Plates, *Applied Mathematics and Mechanics-English Edition*, vol. 34, pp. 1177–1186, 2013.
22. E. Reissner, The Effect of Transverse Shear Deformation on the Bending of Elastic Plates, *Journal of Applied Mechanics*, vol. 12, pp. 69–77, 1945.
23. W. Yuan, X. Wang, H. Song, and C. Huang, A Theoretical Analysis on the Thermal Buckling Behavior of Fully Clamped Sandwich Panels with Truss Cores, *Journal of Thermal Stresses*, vol. 37, pp. 1433–1448, 2014.
24. W. Yuan, H. Song, X. Wang, and C. Huang, Experimental Investigation on Thermal Buckling Behavior of Truss-Core Sandwich Panels, *AIAA Journal*, vol. 53, pp. 948–957, 2015.
25. V. S. Deshpande, N. A. Fleck, and M. F. Ashby, Effective Properties of the Octet-Truss Lattice Material, *Journal of the Mechanics and Physics of Solids*, vol. 49, pp. 1747–1769, 2001.
26. S. Hyun, A. M. Karlsson, S. Torquato, and A. G. Evans, Simulated Properties of Kagome and Tetragonal Truss Core Panels, *International Journal of Solids and Structures*, vol. 40, pp. 6989–6998, 2003.
27. H.-S. Shen, *A Two-step Perturbation Method in Nonlinear Analysis of Beams, Plates and Shells*, John Wiley & Sons, New York, 2013.